RSC Advances

ROYAL SOCIETY OF CHEMISTRY

www.rsc.org/advances

Graphical abstract

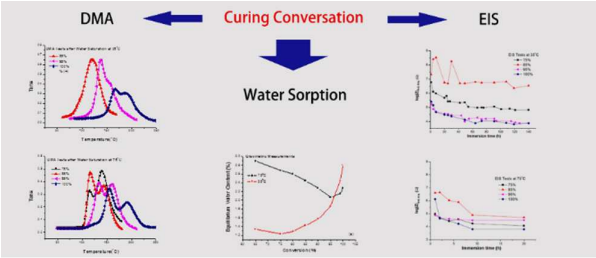

Thermal mechanical properties and corrosion resistance of epoxy resin showed extensive relationship with curing conversion, which showed an optimized performance regime at curing conversion close to ca. 85% due to the balanced property of water sorption and crosslink density

RSC advances

RSCPublishing

ARTICLE

Effect of Curing Conversion on the Water Sorption, Corrosion Resistance and Thermo-Mechanical Properties of Epoxy Resin

Huiping Wang, Yi Liu, Jie Zhang, Tian Li, Zhongnan Hu, Yingfeng Yu *

Cite this: DOI: 10.1039/x0xx00000x

Received 00th January 2012,
Accepted 00th January 2012

DOI: 10.1039/x0xx00000x

www.rsc.org/

Study of the relationship between curing conversion and properties is critical for optimizing the performance of epoxy materials. In this article, the change of thermo-mechanical and corrosion resistance properties of diglycidyl ether of bisphenol A/ diaminodiphenylsulfone epoxy system with curing conversion were studied by various instruments. The water sorption process showed an opposite trend of equilibrium water content with curing conversion at high and low temperatures, which was found to be related to different mechanisms by infrared spectroscopy study. The mechanical tests and corrosion resistance (EIS) experiments showed an optimized performance region at curing conversion close to ca. 85%.

1. Introduction

With the rapid developments of aerospace and microelectronics technologies, epoxy resins as the structural and packaging materials are required to possess even better performance in recent years than ever before. Beside the research of novel high performance epoxy systems, optimization of the properties of existing epoxy materials through processing and structure-property study is another effective route to improve the performance of materials.

In previous works[1-4], the thermo-mechanical properties of epoxy resin with different curing conversions have been carefully studied, however, most of the results are somehow inconsistent with each other[5-8]. While few work reported the relationship between corrosion resistance and curing conversion.

With various polar groups like hydroxyl and amino groups, epoxy resins are vulnerable to absorbing water and thus leading to a catastrophe on properties like mechanical properties and corrosion resistance. Water molecules could transport to the resin matrix and metal-resin interface and lead to performance loss when epoxy resin is used as coating or adhesive in various application fields.

For epoxy coatings, Shreepathi et al[9] found that equilibrium water content was an important factor of corrosion resistance, for coatings with lower equilibrium water content showed better corrosion resistance through electrochemical impedance spectroscopy (EIS) and salt spray exposure test. Kamisho et.al[10] gave a similar result and suggested that equilibrium water content affected adhesive performance much more than diffusion coefficient. Liu et.al[11] further demonstrated that increasing crosslink density could improve the corrosion resistance of the coatings. Clearly, understanding the water sorption mechanism is crucial for the corrosion resistance of epoxy resins.

Water molecules that diffuse in epoxy network may act as a diluent and thus lead to a loss on properties[12]. However, Macqueen et al[13] found that the free volume of epoxy resin decreased after water sorption, which may result from the anti-plasticizing effect of water molecules occupying the original free volume of epoxy resin. While Choi et al[14] observed Tg increased after water sorption due to additional curing of epoxy during this process.

To well organize the above contradictory results, hydrogen bond theory was then applied for explaining the interaction between epoxy and water molecules[15-21]. Three types of water molecules may exist depending on their interactions with epoxy: without hydrogen bond (S_0); with one hydrogen bond (S_1); and with double hydrogen bonds (S_2). S_0 and S_1 water molecules work as plasticizer, and S_2 works as anti-plasticizer. Two-Dimensional (2D) ATR-FTIR spectroscopy was further well used [22-26] with combination of the hydrogen bond theory for the study of water diffusion in epoxy resins at low temperature.

In our previous works[26-28], we found that the polarity and free volume are the most important factors influence water sorption in epoxy resin. Polarity is the primary factor determining equilibrium water content, while free volume mainly affects diffusion coefficient. As for the water sorption

with different curing conversions, Nogueira et.al[12] found that epoxy resins with higher conversion have larger equilibrium water content at low temperature for highly polar structure. While the result from Enns et.al[29] shows that the equilibrium water content of epoxy resins increased with increasing curing conversion at room temperature due to more free volume. Frank et.al[30] gave a similar result. However, few researches have systematically studied the effect of curing conversion on properties of epoxy resins, and the corrosion resistance with water diffuse behaviour at both high and low temperatures.

In this work, we chose one of the most well-used epoxy systems, diglycidyl ether of bisphenol A/diaminodiphenyl-sulfone (DGEBA/DDS), as the model to study the relationship between curing conversion and thermo-mechanical, water sorption, and corrosion resistance properties. The results would be helpful for understanding corrosion resistance performance and properties change of epoxy materials with curing procedure.

2. Experimental

2.1 Material

Diglycidyl ether of bisphenol A epoxy resin (DGEBA)(DER 331,Dow chemical Co. epoxy value, 0.51-0.55 mol/100g epoxy), the curing agent 4,4'-diamino-diphenylsulfone (DDS) was manufactured by the Sinopharm Chemical Reagent Co.(Shanghai,China). The chemical structures of DGEBA and DDS are illustrated in scheme 1.

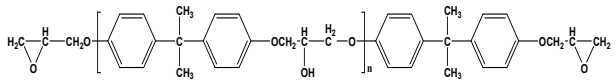

DGEBA

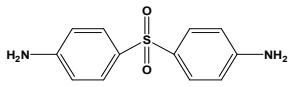

DDS

Scheme 1

Specimen preparation

Samples were prepared by dissolving the curing agents in epoxy resins in a stoichiometric epoxy/amine molar ratio at 150°C, and then cured for different time as showed in Table 1, in which the curing conversions were monitored by Near-IR with a deviation of ca. 2%. The curing procedures of different curing conversions were performed on the basis of iso-thermal DSC study.

2.2 Experimental Techniques

Different Scanning Calorimetry (DSC)

Calorimetric analyses were carried out on a Mettler DSC-823e thermal analyzer. Samples of approximately 5 mg in weight were cured in aluminium pans in nitrogen atmosphere. In the isothermal and dynamic curing process, the degree of conversion by DSC was calculated as follows:

Table1. Curing conditions for different curing conversions

Curing conversion	Curing condition
65%	150°C for 1.5 hours
75%	150 °C for 2 hours
80%	150 °C for 2.5 hours
85%	150 °C for 3 hours
90%	150 °C for 4 hours
95%	150 °C for 6 hours
99%	150 °C for 2 hours & 180 °C for 3hours
100%*	150 °C for 2 hours & 180 °C for 3hours & 200 °C for 4 hours

*: fully post cured, the conversion near to 100%

$$\alpha_{DSC} = \frac{\Delta H_t}{\Delta H_{total}} \quad (1)$$

Where ΔH_t is the heat released up to a temperature T obtained by integration of the calorimetric signal up to this temperature in the dynamic process, while for isothermal curing it corresponds to a curing time t, and ΔH_{total} is the total reaction heat associated with the complete conversion of all reactive groups.

Dynamic Mechanical Analysis (DMA)

The dynamic mechanical properties were collected with a Netzsch DMA 242 operating in the double cantilever mode at an oscillation frequency of 1Hz. The specimens for DMA were prepared in the form of cuboid bars with nominal dimension of 30 ×10 ×1 mm. The data were collected from 50°C to 250 °C at a scanning rate of 3 °C /min.

Mechanical test

The Izod impact test was performed at room temperature (RT) by means of an Izod 5110 impact tester, according to ISO 180-2000 using unnotched rectangular specimens. The pendulum employed had a kinetic energy of 1 J. The impact strength was obtained by taking the average values of ten specimens.

The T-peel adhesion strength between copper foil and epoxy composites were using an Instron Model 5565 universal tester according to IPC-650-650 standard at RT temperature. Each test reported was the average of at least five sample measurements.

Gravimetric measurements

The Sample sheets (10mm×10mm×1mm) were polished with distilled water and then dried under vacuum oven at 100 °C for 24 h. Water sorption at 35 °C and 75 °C was then monitored in the resins as a function of immersion time. The samples were periodically removed from the water, wiped down and quickly weighed on a Tg332A microbalance (accuracy, 0.01mg). The water sorption (content at time t, M_t) of the sample is achieved as below:

$$M_t = \frac{W_t - W_0}{W_0} \times 100\% \quad (2)$$

Where W_0 is the weight of the dry specimen, and W_t is the weight of the wet specimen at time t.

RSC advances RSCPublishing

ARTICLE

Diffusion Measurements by Time–Resolved ATR-FTIR

All time-resolved ATR-FTIR measurements were performed at 35 ^{o}C using a Nicolet Nexus Smart ARK FTIR spectrometer equipped with a DTGS-KBr detector, solid cell accessories, and a ZnSe internal reflection element (IRE) crystal. The spectra were measured at 4 cm^{-1} resolution and 32 scans, with the wavenumber range being 2700-3700 cm^{-1}. The film-covered IRE crystal with a filter paper above the sample film was mounted in an ATR cell, and the spectra of the dry film were collected as background spectra. Afterwards, without moving the sample, distilled water was injected into the filter paper while starting the data acquisition by a macro program. The thickness of the films was about 15mm.

Diffusion Measurements by Near-IR

Samples with different curing conversions were immersed in distilled water at 75 ^{o}C, and near-IR transmission spectra were recorded at selected time intervals during the immersion. The near-IR spectra, at 4 cm^{-1} resolution and 128 scans, were then obtained using the Nicolet Nexus 470 with a white light source and an MCT detector. The thickness of the samples was about 5 mm.

Two Dimensional (2D) Correlation Analysis.

A series of spectra at equal time intervals in certain wavenumber ranges was selected for a 2D correlation analysis using the 2D Shige software. Time-averaged reference spectrum was shown at the side and the top of the 2D correlation maps for comparison. In the 2D correlation maps, red regions indicated positive correlation intensities, while blue regions indicated negative correlation intensities.

Electrochemical impedance spectroscopy (EIS) measurements

EIS measurements for the epoxy-coated metal systems were performed on a CH650E electrochemical workstation (Shanghai Chenhua Instruments Inc., China) in 3.5wt% NaCl solution by using three-electrode system. An epoxy-coated stainless steel acts as the working electrode, the thickness of the coatings was about 100μm, a saturated calomel electrode (SCE) as the reference electrode and platinum sheet electrode (15*15mm) as the counter electrode. The coating area exposed to the electrolytic solution was 1.7671cm^2 (R=1.5cm). All the measurements were carried out at open circuit voltage by applying a sinusoidal voltage of 5 mV and the spectra were recorded in the frequency range of 0.1Hz to 1000 kHz.

3. Results and discussion

3.1. Effect of curing conversion on the thermo-mechanical properties

Increase of curing conversion enhances thermal transitions of epoxy resins like glass transition temperature (T_g) due to the change of crosslink density and free volume. T_g as a function of conversion was reported by many authors[2,31,32]. DMA is a powerful method for characterizing the relationship of T_g and curing conversion[1,33].

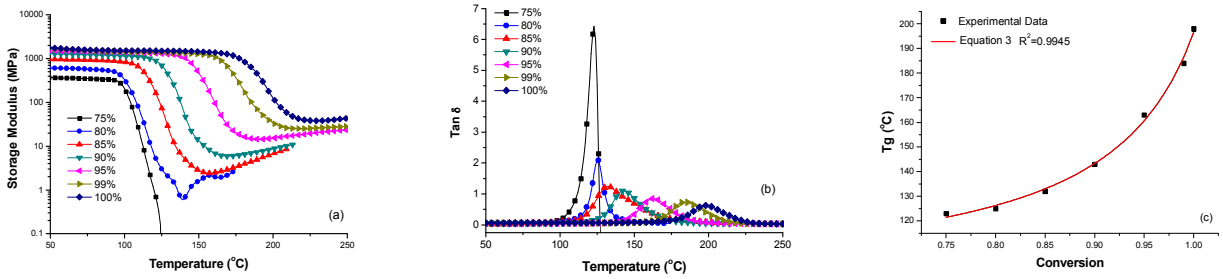

Fig. 1. Effect of curing conversion on the thermo-dynamic properties of DGEBA-DDS: (a) storage modulus; (b) α transition; (c) T_g versus conversion

Figure 1 shows the DMA study of DGEBA-DDS system with different curing conversions. Both storage modulus and tanδ increased as curing conversion increased, and the enlargement of storage modulus after T_g transition suggests the increase of crosslink density. In this study, the peak temperature of tanδ is defined as glass transition temperature. The T_g versus conversion data is shown in Figure 1c, in low conversion region, T_g versus conversion exhibits an approximate linear relationship due to chain-end concentration decrease, but T_g increased sharply in high conversion region resulting from combination of chain-end concentration decrease and crosslink density increase[2]. This T_g-conversion relationship is consistent with other reports of epoxy resins[2,33]. The T_g-conversion relationship has been studied in numerous

works[2,32,34,35], and the DiBenedetto equation has been well accepted:

$$\frac{T_g - T_{g0}}{T_{g\infty} - T_{g0}} = \frac{\lambda\alpha}{1-(1-\lambda)\alpha} \quad (3)$$

Where α is the curing conversion, T_{g0} is the T_g of unreacted monomers mixture, $T_{g\infty}$ is the T_g of fully cured thermoset, λ is the ΔC_p values of the fully cured and unreacted materials.

By fitting the experimental data into Eq. 3 shown as a red line in Figure 1c, it can be found that the equation can well describe the T_g-conversion relationship with a square error of R^2=0.995.

The mechanical properties of epoxy resin with different curing conversions were tested to evaluate their relationship as shown in Figure 2. Figure 2a shows the impact strength of samples with different curing conversions. With the increase of curing conversion, the impact strength increased at the same time initially. Especially at 85%, the impact strength increased dramatically, nearly twice the value of 80%. After 90%, the impact strength changed little, even decreased at 95% and 100%, i.e. the impact strength levelled off when curing conversion was above 85%.

The influence of curing conversion on the average peeling strength of the epoxy resin using both unoxidized and oxidized (with black oxide layer) copper foil shown in Figure 2b. Maximum values appear at conversion between 80% and 95% both in unoxidized copper clad and oxidized copper clad. It is generally accepted that peel strength is highly dependent on the adhesive strength of the copper-resin interface and the flexibility of matrix resin. In other words, the peel strength is closely related to the toughness of the materials.

With the increase of curing conversion, more epoxy groups are polymerized or reacted with curing agents, which increases the crosslink density and lowers down the chain mobility of epoxy networks, thus results in higher modulus, higher tensile strength and lower elongation at break. Therefore, it can be easily inferred that there would be a highest value of peel strength at a specific curing conversion (not 100%) based on factors mentioned above. This deduction is confirmed by our previous study[1], which demonstrated that the maximum peel strength is located at about 80-95% curing conversion.

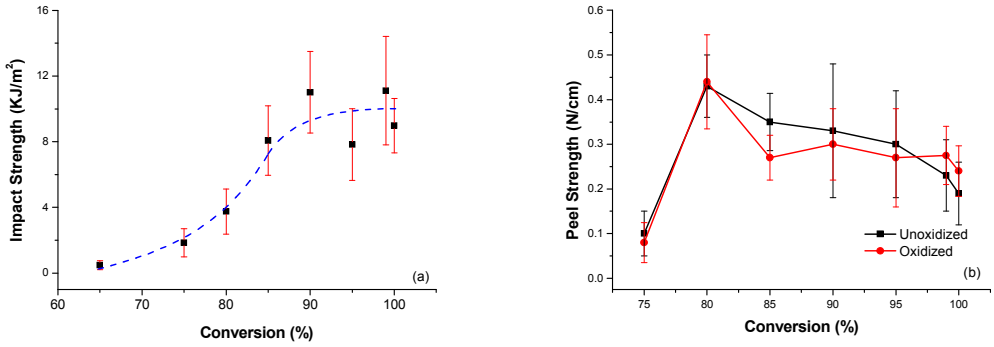

Fig. 2. Mechanical tests of epoxy resin with different curing conversions. (a) impact strength; (b) peeling strength between copper foil and epoxy resin.

3.2 Water sorption

Beside thermal and mechanical properties, the curing conversion would also have deep impact on the corrosion resistance and stability of epoxy materials. And water sorption is a critical property which is closely related to the performances mentioned above.

Gravimetric Measurements

As epoxy materials were widely used in various industrial areas, two temperatures, 35°C and 75°C, were selected to study the water sorption behaviour as a simulation of normal RT and high temperature applications. Figure 3 shows the gravimetric measurements of water sorption at 35°C and 75°C, and the equilibrium water contents (M_∞) with different curing conversions obtained from this test are shown in Figure 4a. At 35°C, equilibrium water content increased with conversion. However, a quite different tendency was observed at 75°C: equilibrium water content first decreased with the conversion, then increased again after reaching the lowest value at 95%. Another curious result is the lower water sorption content of 99% and 100% samples at high temperature, which cannot be simply explained by previous knowledge. To discover the root cause of this kind of unusual water sorption difference at high and low temperatures, we chose IR and DMA instruments to monitor the water sorption process, which will be discussed in the next part of this article.

In another aspect, diffusion coefficient is an important index affects the properties of epoxy materials. It is generally accepted that the behavior of water sorption curves in epoxy conforms to Fickian diffusion in the initial sorption process. The diffusion coefficients fulfill the following equation according to Fick's second law[36]:

$$\frac{M_t}{M_\infty} = \left(\frac{4}{L\sqrt{\pi}}\sqrt{D}\right)\sqrt{t} \quad (4)$$

RSC advances RSCPublishing

ARTICLE

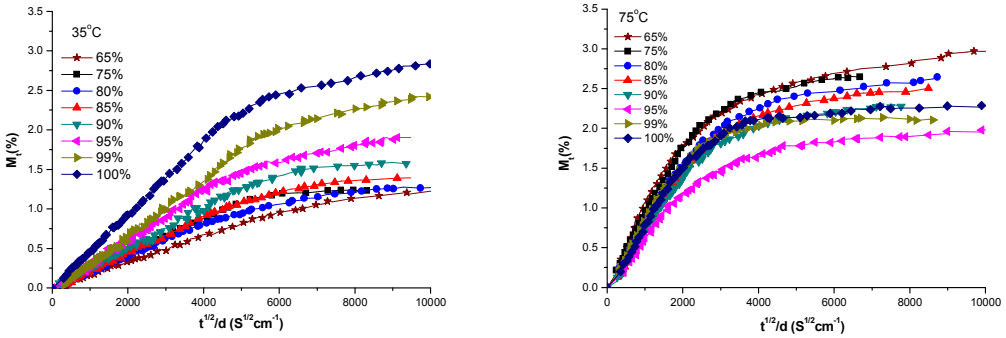

Fig. 3. The gravimetric results of water sorption at 35°C and 75°C.

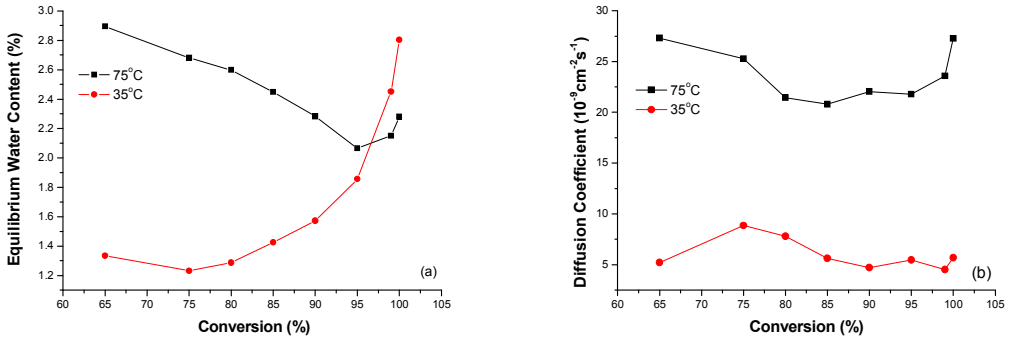

Fig. 4. Equilibrium water content (a) and Diffusion coefficient (b) versus curing conversion at 35°C and 75°C.

Where and M_t is water sorption at time t, M_∞ is the equilibrium value of the diffusing water at infinite time, D is the diffusion coefficient, L is the thickness of the specimen.

Diffusion coefficients were calculated from the initial slope of these sorption curves by curve fitting according to Eq. 4, the fitting curve of water diffusion of 65% at 35°C is shown in Figure 5 as an example. Figure 4b displays the diffusion coefficient versus curing conversion at 35°C and 75°C. Diffusion coefficient decreased first with curing conversion (reached the lowest values at 85%-95% region) and then increased.

In previous works[26], it was found that the diffusion coefficient is mainly controlled by free volume, while polarity has minor effect on diffusion coefficient. With the increase of curing conversion, free volume decrease that restricts the arrangement of backbone and segments of epoxy networks. Because of the increase of T_g and enlargement of crosslink density resulting from the reaction of epoxy and amine groups. However, further curing lead to fractional free volume increase[37-39] As a result, diffusion coefficient first increased with curing conversion, then decreased when epoxy was near fully cured. At high temperature as 75°C, more free volume exists compared to that at lower temperature. So high temperature favors the chain/segment disentanglement, and the diffusion coefficient has a higher value.

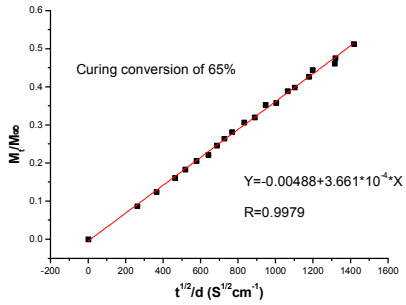

Fig. 5. The fitting curve of water diffusion of curing conversion 65% at 35°C

This contrary change of equilibrium water content may suggest a different water sorption mechanism at high and low temperatures. In order to well understand the diffusion mechanism of water sorption at high and low temperatures and the effect of water sorption on other properties, we therefore selected specimens of conversion of 75%, 85%, 95%, and 100% as representations for other instrument tests.

Diffusion behaviour at 35°C

The ATR-IR spectrums of water diffusion in DGEBA-DDS system at 35°C are shown in Figure 6, in which the IR spectra of absorbed water in the range of 3700-2800cm^{-1} reveals an increasing intensity of OH vibration band(located at 3700-3000cm^{-1}) as water diffuses into epoxy networks.

2D correlation analyses were performed to study the water diffusion behaviour due to its significant advantages[40]: 1) it has a higher distinguishability than one-dimensional spectrums thus can distinguish some weak peaks which are hard to be detected by one-dimensional spectrums; 2) it is able to observe the specific sequence of certain events taking place in the system. The 2D correlation spectrums in the range of 3700-3000 cm^{-1} are shown in Figure 7. In synchronous spectrums only one strong auto-peak was observed at 3400cm^{-1}, which is assigned to OH stretching band of water molecules. While more information can be obtained from the corresponding asynchronous correlation spectrums. Take the asynchronous correlation spectrum of 100% as an example, two cross-peaks $\Psi(3400,3172)<0$, $\Psi(3610,3172)<0$) dominate the asynchronous map in the upper left triangle of this figure, which suggests there are three species of water molecules, located around 3610, 3400, and 3172cm^{-1}, respectively.

In the research of water diffusion in polar polymer systems, four sorption peaks located in 3600 cm^{-1},3500 cm^{-1},3400 cm^{-1} and 3200 cm^{-1} were found through infrared spectrum peak fitting method[19,41-43]. Musto et al[19,44] assigned the four bands to water molecules without hydrogen bond (S_0, 3600cm^{-1}), with one hydrogen bond (S_1, 3500cm^{-1}), and with double hydrogen bonds (loosely bonded S_{2L} ,3400cm^{-1}; and tightly bonded S_{2T} 3200cm^{-1}). The difference of S_{2L} and S_{2T} is resulted from the different strength of the hydrogen bonds.

According to Noda's rule[40], if $\Phi(\nu_1,\nu_2)>0$, $\Psi(\nu_1,\nu_2)>0$, band ν_1 will vary prior to band ν_2, and if $\Psi(\nu_1,\nu_2)<0$, band ν_1 will vary behind to band ν_2. In the asynchronous correlation spectrum of 100%, Ψ (3400, 3172) <0, Ψ (3610, 3172) <0, which indicate that the change of S_{2T} is always sooner than the change of S_0, S_{2L}. The results of 2D correlation analysis for ATR-IR were summarized in Table 2, bond water molecules such as S_{2T} or S_{2L} changed prior to S_0.

Previous studies have demonstrated that water sorption in epoxy resins is controlled by two factors: polarity and free volume; the former one endows hydrogen bonding sites for water molecules, while the latter one provides path for water diffusion. In other words, the competition and coordination of these two factors decide the water sorption in epoxy resins. During the curing process, each primary amine group reacts with an epoxide group to form a linkage with one secondary amine group and one hydroxyl group; further reaction of secondary amine with epoxide generates a tertiary amine and another hydroxyl group. In other words, with the increase of curing conversion, polarity of epoxy resin enlarges quickly at the same time. As for the water sorption at low temperature as 35°C, which is far below the T_g of epoxy resins, chain/segment rotation is essentially frozen while only vibration of side group exists. So polarity is the primary factor deciding the equilibrium water sorption of epoxy resins. With the increase of curing conversion, there would be more polar sites for water molecules to form hydrogen bonds. Thus the equilibrium water content increased with curing conversion.

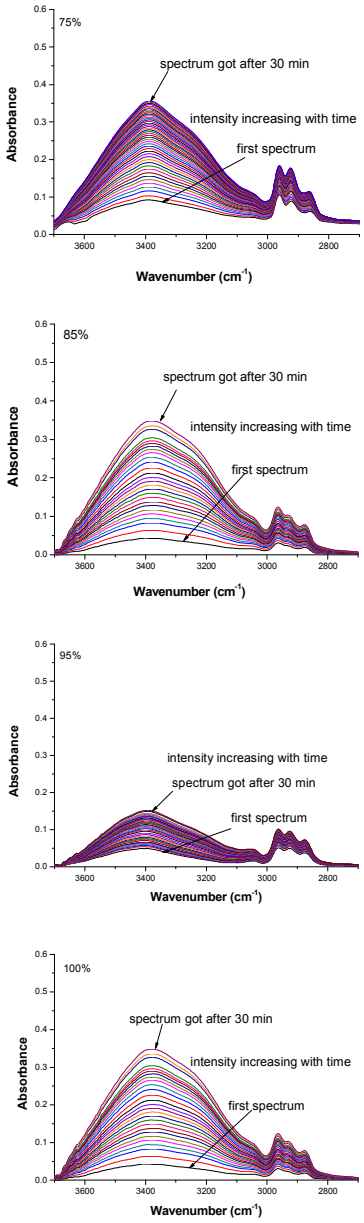

Fig.6. The spectrums of water diffusion in DGEBA-DDS system at 35°C

RSC advances RSCPublishing

ARTICLE

Table 2. The Results of 2D correlation analysis for ATR-IR

Curing conversion	Synchronous spectrum	Asynchronous spectrum	Diffusion order
75%	Φ(3380,3380)	Ψ(3660/3440)<0, Ψ(3440/3230)>0	$S_{2L}>S_0$, S_{2T}
85%	Φ(3360,3360)	Ψ(3410/3172)<0	$S_{2T}>S_{2L}$
95%	Φ(3385,3385)	Ψ(3610/3410)<0, Ψ(3410/3220)>0,	$S_{2L}>S_0$, S_{2T}
100%	Φ(3375,3375)	Ψ(3610/3172)<0, Ψ(3400/3172)<0,	$S_{2T}>S_0$, S_{2L}

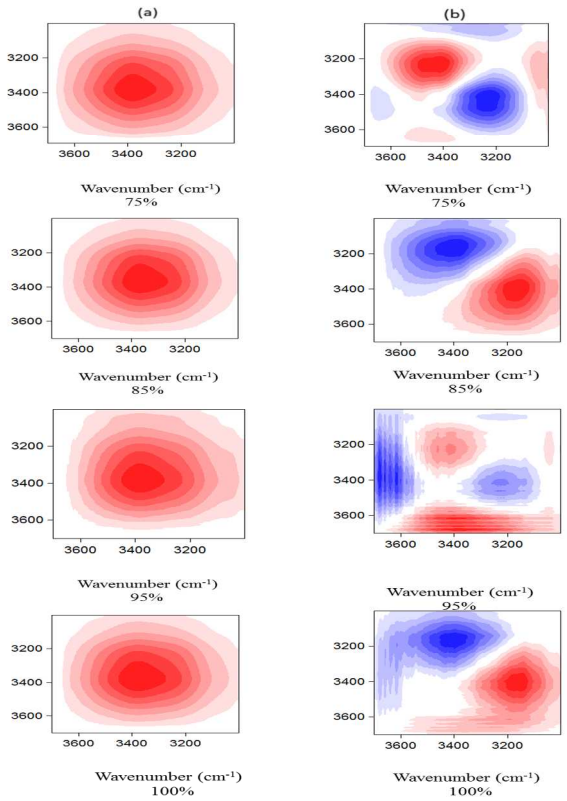

Fig.7. 2D correlation spectrums of water diffusion of DGEBA-DDS at 35 °C : (a) synchronous spectrum; (b) asynchronous spectrum

Diffusion behaviour at 75°C

Clearly, the diffusion mechanism at 35°C cannot explain what happened at 75°C. To investigate the behaviour of water diffusion at high temperature, NIR experiments were performed at 75°C. In Figure 8, the IR spectrums of absorbed water in the range of 7300-6300cm^{-1} and of 5400-4800cm^{-1} reveal an increasing intensity of OH stretching vibration band (located at 7300-6300cm^{-1}) and of OH bending vibration band (located at 5400-48000cm^{-1}) as water diffuses into epoxy networks. In the region of 7300-6000 cm^{-1}, the absorbance of three separate bands located around 7070, 6810, and 6560 cm^{-1} increased with time in the subtracted spectrums (Figure 8b) of 75% and 85%. The results agreed well with Buijs and Musto's studies[15,17], in which they assigned the stretching vibration peaks at 7080 cm^{-1} to S_0, 6800cm^{-1} to S_1, and 6535 cm^{-1} to S_2, respectively. However, only two bands located around 7070, 6810 cm^{-1} were observed for 95% and 100%, which might indicate that there were no S_2 water molecules in 95%, 100% samples.

2D correlation analysis was applied for the water diffusion at 75 °C as shown in Figure 9. In Figure 9a, there are three auto-peaks in 75% and 85%, located at 7080, 6810, and 6560 cm^{-1}, respectively. While only two auto-peaks, located at 7080 and 6810cm^{-1} in 95% and 100%. The results indicate that three types of water molecules (S_0, S_1, and S_2) were observed in 75% and 85%, while only two types (S_0 and S_1) for 95% and 100%, which agree with the subtracted spectrums. In the asynchronous spectrum of OH stretching region, the peak of S_0 was split into two peaks: 7100, 7000cm^{-1} . One can find that the band located at high frequency shifted to higher frequency with water diffusing into epoxy resin, suggesting blue-shift occurred at the OH stretching region shown in Figure 8b. The 2D correlation analysis for NIR was summarised in Table3. Clearly, S_0 changed prior to S_1 and S_2 at 75°C, which is reverse to the sequence of water sorption at 35°C.

When water sorption took place at high temperatures (75°C), both chain/segment disentanglement and vibration of side group are possible. In this case, as the epoxy group showed no change during the water sorption process, i.e., no chemical reaction takes place with the aid of water, we deem that water sorption is a result of chain rotation and hydrogen bonds forming process. The reorientation of epoxy network first favour the diffusion of free water molecules through free volumes, and then chain ends further connect with diffused water molecules to form amine-water-amine (hydroxyl and epoxy) hydrogen bonds. From this point of view, one can expect that large amount of chain ends with unreacted secondary/primary amine groups and epoxy groups would be more possible to form hydrogen bonds with water molecules. Thus, with the increase of curing conversion, the equilibrium water content decrease.

The tendency turned at ca. 95% may come from two reasons: (1) chain mobility drops greatly with curing conversion as the sharp increase of T_g; (2) the amount of chain ends with unreacted groups decreases quickly when epoxy is near fully-cured. Therefore, the equilibrium water content showed larger values in low conversion region due to the physical-crosslinking consumed water; while getting larger again at 100% due to higher polarity and larger free volume.

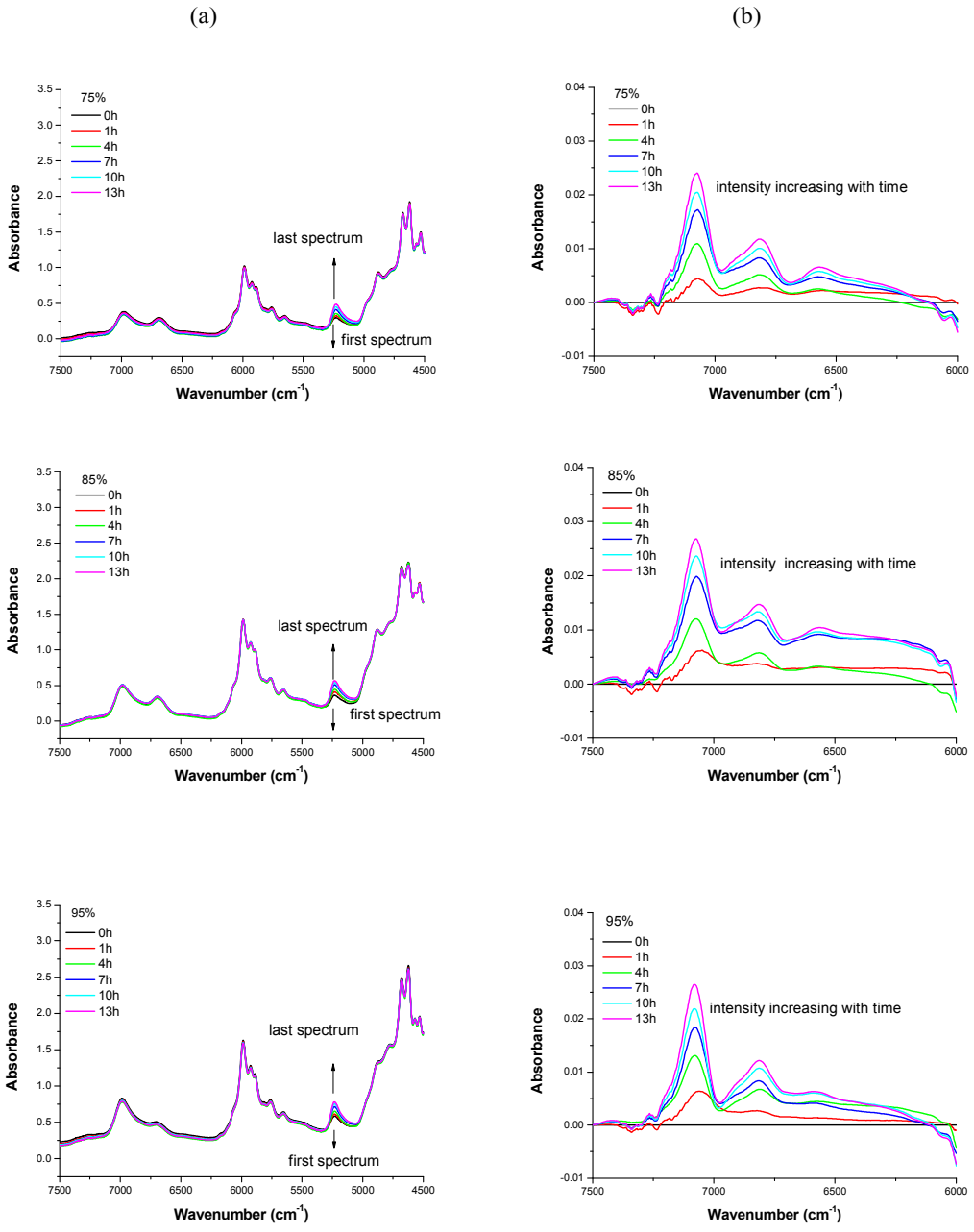

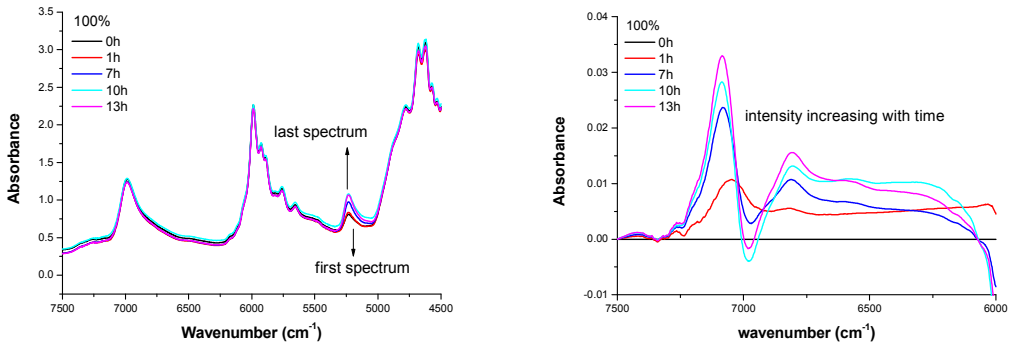

Fig. 8. Near-IR spectra of water diffusion in DGEBA-DDS at 75°C: (a) original spectrums; (b) subtracted spectrums

Table 3. The Results of 2D correlation analysis for NIR

Curing conversion	Synchronous spectrum		Asynchronous spectrum	Diffusion order
	Auto-peak	Cross-peak		
75%	Φ(7080,7080), Φ(6810,6810), Φ(6560,6560)	Φ(7080,6810)>0, Φ(7080,6560)>0, Φ(6810,6560)>0	Ψ(7000,6560)>0, Ψ(7000,6810)>0	$S_0>S_1$;$S_0>S_2$
85%	Φ(7080,7080), Φ(6815,6815), Φ(6560,6560)	Φ(7080,6815)>0, Φ(7080,6560)>0, Φ(6810,6560)>0	Ψ(7000,6560)>0,Ψ(7000,6815)>0	$S_0>S_1$;$S_0>S_2$
95%	Φ(7085,7085), Φ(6815,6815),	Φ(7085,6815)>0,	Ψ(7000,6815)>0	$S_0>S_1$
100%	Φ(7085,7085), Φ(6800,6800),	Φ(7085,6800)>0,	Ψ(7000,6800)>0	$S_0>S_1$

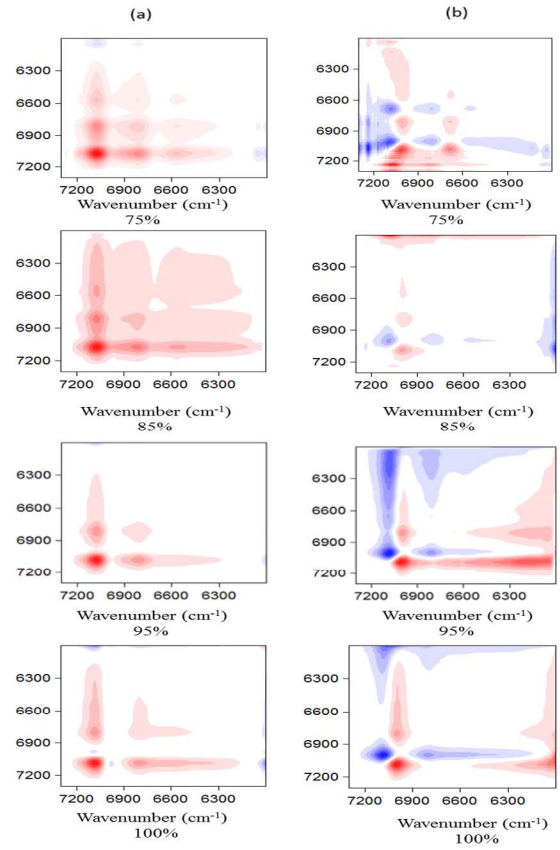

Fig. 9. 2D correlation spectra of water diffusion of DGEBA-DDS at 75 °C: (a) synchronous spectrum of OH stretching region, (b) asynchronous spectrum of OH stretching region.

3.3 Effect of Water sorption on properties

Thermal-mechanical properties

To demonstrate the above hypothesis on the basis of IR study, DMA was used to study the glass temperature of specimens before and after water saturation at 35°C and 75°C as shown in Figure 10. The values of T_g before and after water saturation were summarized in Table 4.

Significant differences were observed in both cases as T_g changed dramatically after water sorption. After water sorption at 35°C, T_g drops about 10~30 °C due to the plasticization effect of water molecules in epoxy network, which mainly resulted from the destruction of intramolecular hydrogen bonding in epoxy. With the increase of water sorption content, the decrease of T_g enlarged with curing conversion from 12 °C for 75% to 30 °C for 100%.

However, a quite different tendency of T_g change was observed for the systems after water sorption at 75°C. Two T_gs were confirmed as tanδ spilt into two peaks for all samples. The first T_g resemble to what observed for system after water sorption at 35°C, which can also be attributed to plasticization effect caused by water molecules. Whereas, the second T_g located at higher temperature showed interesting variations. Comparing with the T_g of epoxy before water sorption, the

second T_g of sample 75% and 85% increased, while the T_gs of sample 95% and 100% decreased ca. 6°C. This kind of T_g increase for sample 75% and 85% clearly results from the physical crosslinking of water molecules with chain ends (or functional groups) through hydrogen bonds, which makes little change of curing conversion since epoxy groups show minor changes during water sorption process. The strength of hydrogen bonding would decrease with the increase of temperature, and dramatically decrease when the temperature is beyond Tg [45-49]. In our study, the T_g of epoxy resins is quite larger than 75°C, therefore, the effect of hydrogen bonding strength with temperature could be minimized. For high curing conversion such as 95% and 100%, the hydrogen bond is looser than chemical bond between amine and epoxy. Therefore, T_g drops a little, which is quite different from the plasticization effect of water as the latter causes more substantial T_g decline.

The results from DMA study before and after water sorption at high and low temperatures could verify the speculation from IR study. At high temperature as 75°C, the chain reorientation favours the sorption of water and the formation of hydrogen bonds. Chain disentanglement reduces the free energy of water-epoxy system, which results in higher equilibrium water contents compare to that at 35°C. Thus the value of first T_g is a little lower than that of system after water sorption at 35°C.

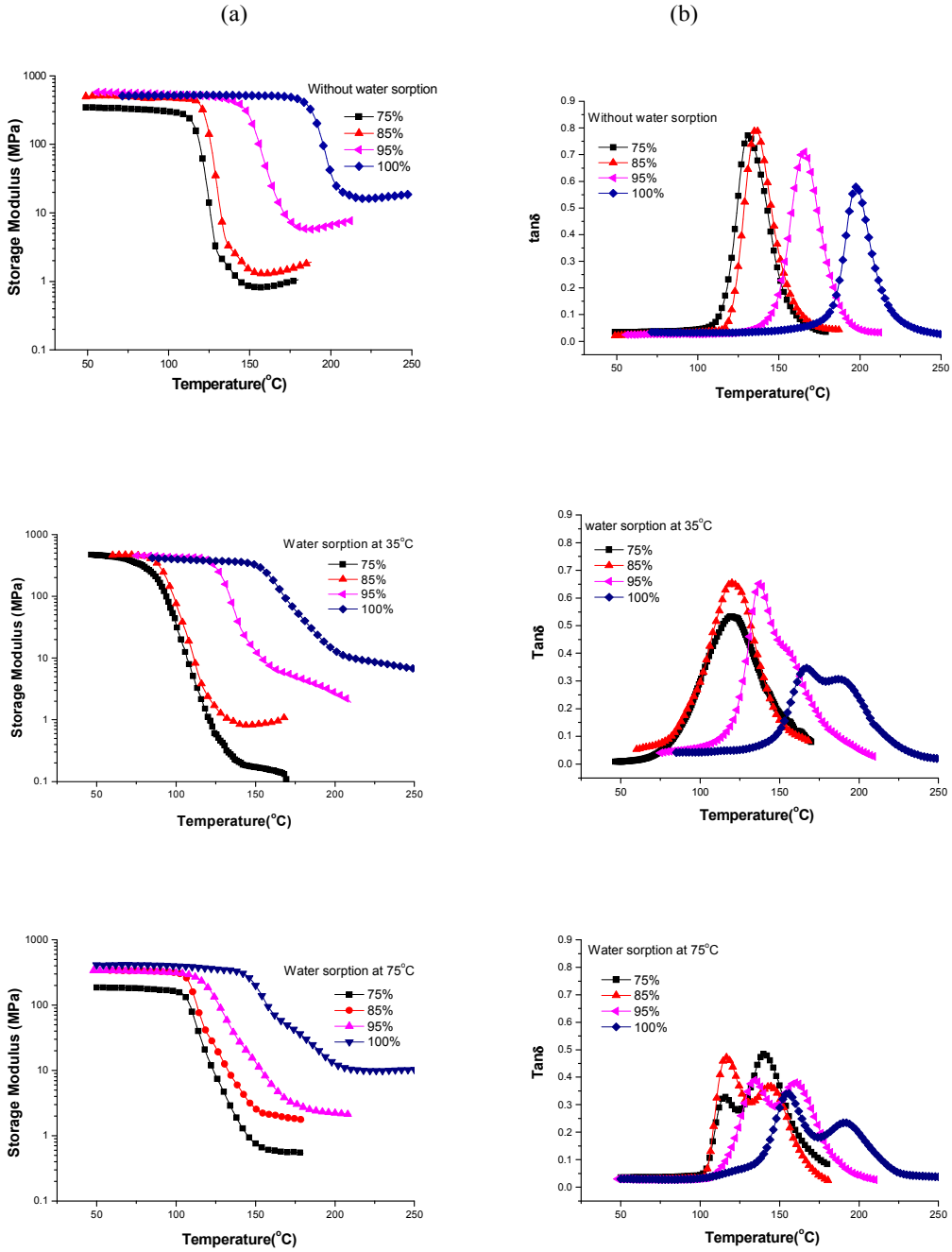

Fig. 10. The DMA curves of DGEBA-DDS before and after water saturation: (a) storage modulus; (b) tanδ

Table 4. The change of T_g (°C) after water saturation at 35°C and 75 °C

Conversion	75%	85%	95%	100%
Dry	131	136	166	197
35°C	119	120	137	167,187
75°C	115,140	116,143	134,160	155,191

Corrosion resistance

As the water sorption shows great dependence on curing conversion at both high and low temperatures, one would expect some differences on the corrosion resistance of epoxy materials as coatings and adhesives.

EIS is widely employed to predict the corrosion resistance of coatings [50-56]. The EIS experiments were performed at 35°C and 75°C respectively. Considering the measuring range of our electrochemical workstation, we keep the thickness of the coatings around 100μm, as a result, the corrosion rate is faster than those systems with thick coatings. Bode plots of EIS spectra with immersion time at 35°C and 75°C are presented in Figure 11.The reduced impedance modulus with immersion time should be attributed to the sorption of NaCl solution by coatings. At 35°C, except 85%, the impedance modulus of 75%, 95% and 100% significantly changed after 20 hours. At high temperature of 75°C, as the thickness of coatings is quite thin, the rate of water diffuses to metal/coating interface is so fast that peeling of coatings occurred only after 9 hours, after that the impedance modulus did not change significantly.

The impedance modulus at low frequency (0.1Hz or 1Hz) is served to estimate the corrosion protection of coated metal[57-59]. In this article, we used the value log|Z| at 0.1 Hz as a function of exposure time to evaluate the corrosion resistance performance of coatings as shown in Figure 12. The impedance modulus decreased faster at 75°C than that at 35°C, as the diffusion coefficient of 75°C was much larger than that of 35°C. For both temperatures, the coating corrosion resistance shows a fluctuation with curing conversion. Better corrosion resistance appeared in the conversion region of 75%-85% for samples at 35°C, and 85%-95% at 75°C. According to literatures[9,10], coatings with lower equilibrium water content show better corrosion resistance. Considering the equilibrium water content from water sorption study, in which the equilibrium water content showed a minimum value corresponding to the corrosion test at both temperatures, i.e. at the curing conversion of 75%-85% and 85%-95%. The primary cause of coating corrosion is water diffuse in the metal-coating interface, so a stronger strength of metal-coating interface would lead to a higher corrosion resistance for coatings. Maximum values of peeling strength appear at conversion between 80% and 95%. Combine the two factors, the conversion of ca. 85% shows the best corrosion resistance.

(a) (b)

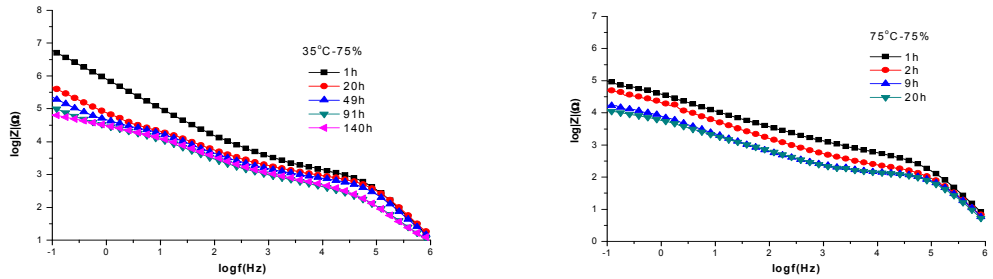

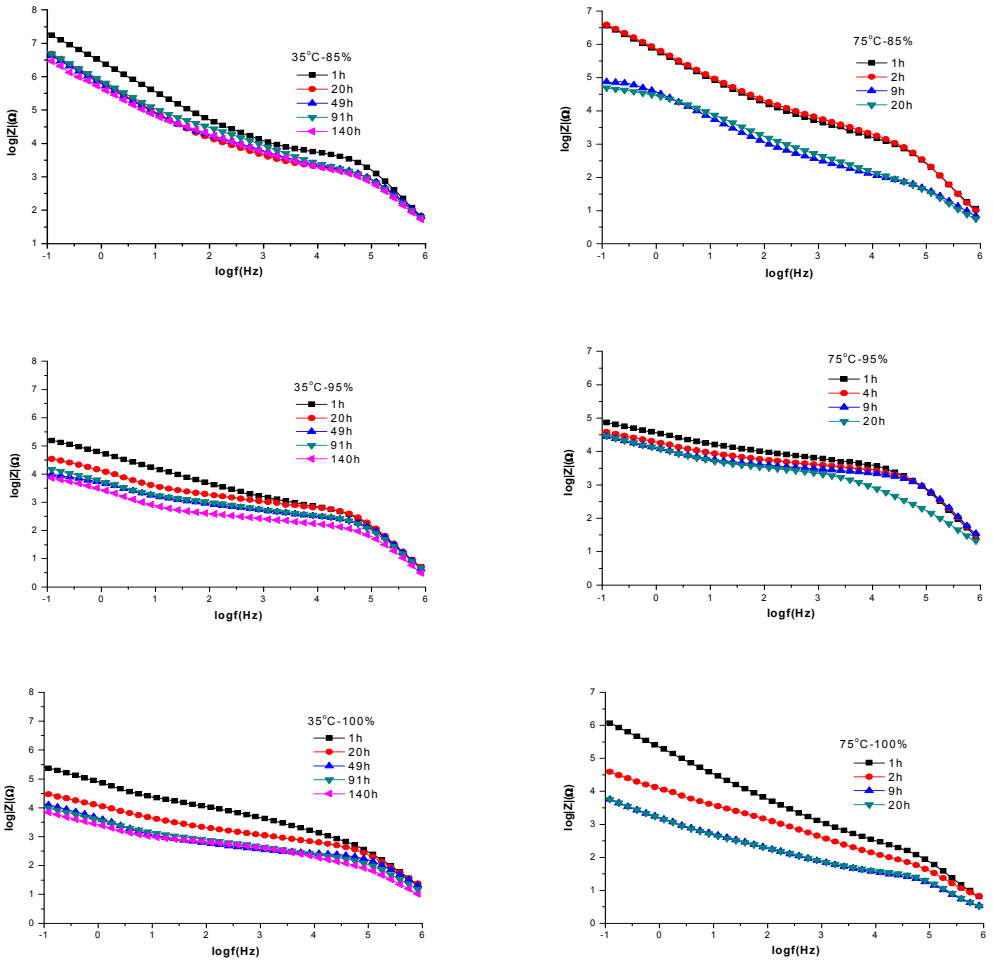

Fig. 11. The Bode plots of EIS spectra, samples were immersed for 1 h prior to measurement: (a)35°C, (b)75°C.

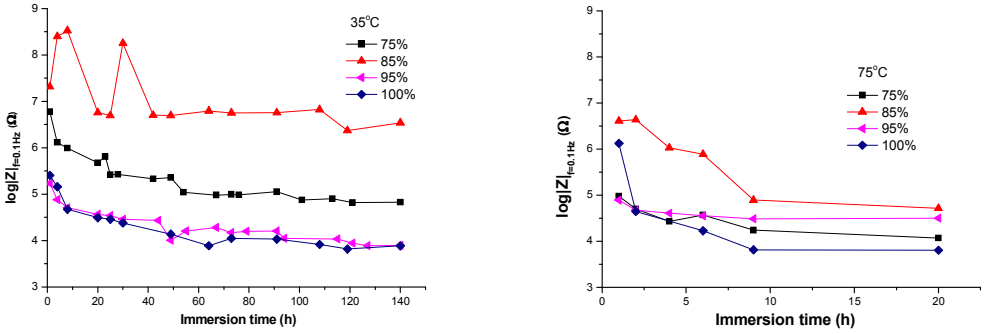

Fig.12. $\log|Z|_{f=0.1\,Hz}$ vs immersion time at 35°C and 75°C.

Conclusion

Curing conversion of epoxy resins showed closely relationship with thermo-mechanical, water sorption, and corrosion resistance properties of materials.

Both the storage modulus and T_g increased with curing conversion, and the growth of T_g with curing conversion could be well described by DiBenedetto equation.

The water diffusion coefficient by gravimetric measurements decreased with curing conversion in low conversion range, and then increased as the free volume change of epoxy, which first

decreases with curing conversion and increases near fully cured.

The equilibrium water content increased with curing conversion at 35°C, but showed a different tendency at 75°C. 2D-dimension IR analysis showed S_2 diffused prior to other types water molecures at 35°C, while free water (S_0) diffused prior to bond water (S_1 and S_2) at 75°C. T_g reduced after water saturation at low temperature, while physical crosslinking took place among water molecules and epoxy resin at 75°C, which resulted in the increase of second T_g in low curing conversion region.

Polarity and free volume influence equilibrum water content. Equilibrium water content at 35°C increased due to the increase of polarity, while the chain disentanglement and hydrogen bonds resulted in a higher water content in low curing conversion region when water sorption at 75°C.

Both mechanical properties and corrosion resistance studied by EIS experiments showed an optimized performance regime at curing conversion close to ca. 85% due to the balanced property of water sorption and crosslink density.

Acknowledgement

This research work was supported by the National Natural Science Foundation of China (Grant 21274031).

Notes and references

State Key Laboratory of Molecular Engineering of Polymers, Department of Macromolecular Science, Fudan University, Shanghai, 200433, China. E-mail:yfyu@fudan.edu.cn; Fax: +86 21 6564 0293; Tel: +86 21 6564 2865.

Reference

1 J. Zhang, T. Li, H. P. Wang, Y. Liu, Y. F. Yu, *Microelectronics Reliability,* 2014, **54**(3), 619-628.
2 A. Hale, C. W. Macosko, H. E. Bair, *Macromolecules,* 1991, **24**(9), 2610-2621.
3 M. J. Marks, R. V. Snelgrove, *Acs Applied Materials & Interfaces,* 2009, **1**(4), 921-926.
4 R. J. C. Carbas, L. F. M. da Silva, E. A. S. Marques, A. M. Lopes, *Journal of Adhesion Science and Technology,* 2013, **27**(23), 2542-2557.
5 J. Jakobsen, M. Jensen, J. H. Andreasen, *Polymer Testing,* 2013, **32**(8), 1417-1422.
6 A. Shokuhfar, B. Arab, *Journal of Molecular Modeling,* 2013, **19**(9), 3719-3731.
7 C. Jordan, J. Galy, J. P. Pascault, *Journal of Applied Polymer Science,* 1992, **46**(5), 859-871.
8 F. Lapique, K. Redford, *International Journal of Adhesion and Adhesives,* 2002, **22**(4), 337-346.
9 S. Shreepathi, S. M. Naik, M. R. Vattipalli, *Journal of Coatings Technology and Research,* 2012, **9**(4), 411-422.
10 T. Kamisho, Y. Takeshita, S. Sakata, T. Sawada, *Journal of Coatings Technology and Research,* 2014, **11**(2), 199-205.
11 M. Liu, X. H. Mao, H. Zhu, A. Lin, D. H. Wang, *Corrosion Science,* 2013, **75**, 106-113.
12 P. Nogueira, C. Ramirez, A. Torres, M. J. Abad, J. Cano, J. Lopez, I. Lopez-Bueno, L. Barral, *Journal of Applied Polymer Science,* 2001, **80**(1), 71-80.
13 R. C. Macqueen, R. D. Granata, *Journal of Polymer Science Part B-Polymer Physics,* 1993, **31**(8), 971-982.
14 S. Choi, E. P. Douglas, *Acs Applied Materials & Interfaces,* 2010, **2**(3), 934-941.
15 K. Buijs, G. R. Choppin, *Journal of Chemical Physics,* 1963, **39**(8), 2035-2041.
16 G. R. Choppin, M. R. Violante, *Journal of Chemical Physics,* 1972, **56**(12), 5890-5898.
17 P. Musto, G. Ragosta, L. Mascia, *Chemistry of Materials,* 2000, **12**(5), 1331-1341.
18 P. Musto, G. Ragosta, G. Scarinzi, L. Mascia, *Journal of Polymer Science Part B-Polymer Physics,* 2002, **40**(10), 922-938.
19 S. Cotugno, G. Mensitieri, P. Musto, L. Sanguigno, *Macromolecules,* 2005, **38**(3), 801-811.
20 G. Mensitieri, M. Lavorgna, P. Musto, G. Ragosta, *Polymer,* 2006, **47**(25), 8326-8336.
21 D. Larobina, M. Lavorgna, G. Mensitieri, P. Musto, A. Vautrin, *Macromolecular Symposia,* 2007, **247**(Times of Polymers and Composites), 11-20.
22 P. Y. Wu, H. W. Siesler, *Chemical Physics Letters,* 2003, **374**(1-2), 74-78.
23 M. J. Liu, P. Y. Wu, Y. F. Ding, G. Chen, S. J. Li, *Macromolecules,* 2002, **35**(14), 5500-5507.
24 L. Li, Y. Chen, S. J. Li, *Applied Spectroscopy,* 2006, **60**(4), 392-397.
25 M. J. Liu, P. Y. Wu, Y. F. Ding, S. J. Li, *Physical Chemistry Chemical Physics,* 2003, **5**(9), 1848-1852.
26 L. Li, Y. Yu, H. Su, G. Zhan, S. Li, P. Wu, *Applied Spectroscopy,* 2010, **64**(4), 458-465.
27 L. N. Li, S. Y. Zhang, Y. H. Chen, M. J. Liu, Y. F. Ding, X. W. Luo, Z. Pu, W. F. Zhou, S. J. Li, *Chemistry of Materials,* 2005, **17**(4), 839-845.
28 L. Li, Y. Yu, Q. Wu, G. Zhan, S. Li, *Corrosion Science,* 2009, **51**(12), 3000-3006.
29 J. B. Enns, J. K. Gillham, *Journal of Applied Polymer Science,* 1983, **28**(9), 2831-2846.
30 K. Frank, J. Wiggins, *Journal of Applied Polymer Science,* 2013, **130**(1), 264-276.
31 J. P. Pascault, R. J. J. Williams, *Journal of Polymer Science Part B-Polymer Physics,* 1990, **28**(1), 85-95.
32 M. Urbaniak, *Polimery,* 2011, **56**(3), 240-243.
33 D. Ren, M. Mills, M. DeGroot, L. Clark, S. Brown, J. Curphy, *Solar Energy Materials and Solar Cells,* 2012, **107**, 403-406.
34 A. T. Dibenedetto, *Journal of Polymer Science Part B-Polymer Physics,* 1987, **25**(9), 1949-1969.
35 R. H. Lin, A. C. Su, J. L. Hong, *Polymer International,* 2000, **49**(4), 345-357.
36 J. Crank, G. S. Park, Diffusion in Polymers, Academic Press, London, 1968, pp Chapter 1.
37 R. A. Venditti, J. K. Gillham, Y. C. Jean, Y. Lou, *Journal of Applied Polymer Science,* 1995, **56**(10), 1207-1220.

38 X. Wang, V. J. Foltz, *Polymer,* 2006, **47**(14), 5090-5096.
39 O. Georjon, J. Galy, *Polymer,* 1998, **39**(2), 339-345.
40 I. Noda, A. E. Dowrey, C. Marcott, G. M. Story, Y. Ozaki, *Applied Spectroscopy,* 2000, **54**(7), 236A-248A.
41 J. X. Zhao, S. J. Deng, J. Y. Liu, C. Y. Lin, O. Zheng, *Journal of Colloid and Interface Science,* 2007, **311**(1), 237-242.
42 M. Ide, D. Yoshikawa, Y. Maeda, H. Kitano, *Langmuir,* 1999, **15**(4), 926-929.
43 C. L. Soles, F. T. Chang, B. A. Bolan, H. A. Hristov, D. W. Gidley, A. F. Yee, *Journal of Polymer Science Part B-Polymer Physics,* 1998, **36**(17), 3035-3048.
44 S. Cotugno, D. Larobina, G. Mensitieri, P. Musto, G. Ragosta, *Polymer,* 2001, **42**(15), 6431-6438.
45 D. Li, J. Brisson, *Polymer,* 1998, **39**(4), 801-810.
46 D. J. Skrovanek, S. E. Howe, P. C. Painter, M. M. Coleman, *Macromolecules,* 1985, **18**(9), 1676-1683.
47 L. Li, G. Yang, *Polymer International,* 2009, **58**(5), 503-510.
48 L. S. Teo, C. Y. Chen, J. F. Kuo, *Macromolecules,* 1997, **30**(6), 1793-1799.
49 Q. Chen, G. Yang, Y. Wang, X. Wu, H. Kurosu, I. Ando, *Journal of Molecular Structure,* 1998, **471**(1-3), 183-188.
50 B. M. Fernandez-Perez, J. A. Gonzalez-Guzman, S. Gonzalez, R. M. Souto, *International Journal of Electrochemical Science,* 2014, **9**(4), 2067-2079.
51 J. J. Santana, J. E. Gonzalez, J. Morales, S. Gonzalez, R. M. Souto, *International Journal of Electrochemical Science,* 2012, **7**(7), 6489-6500.
52 F. L. Floyd, S. Avudaiappan, J. Gibson, B. Mehta, P. Smith, T. Provder, J. Escarsega, *Progress in Organic Coatings,* 2009, **66**(1), 8-34.
53 J. J. Suay, M. T. Rodriguez, K. A. Razzaq, J. J. Carpio, J. J. Saura, *Progress in Organic Coatings,* 2003, **46**(2), 121-129.
54 J. M. McIntyre, H. Q. Pham, *Progress in Organic Coatings,* 1996, **27**(1-4), 201-207.
55 A. Amirudin, D. Thierry, *Progress in Organic Coatings,* 1995, **26**(1), 1-28.
56 F. Mansfeld, *Journal of Applied Electrochemistry,* 1995, **25**(3), 187-202.
57 G. Bierwagen, D. Tallman, J. P. Li, L. Y. He, C. Jeffcoate, *Progress in Organic Coatings,* 2003, **46**(2), 148-157.
58 E. Potvin, L. Brossard, G. Larochelle, *Progress in Organic Coatings,* 1997, **31**(4), 363-373.
59 L. Chen, S. Zhou, S. Song, B. Zhang, G. Gu, *Journal of Coatings Technology and Research,* 2011, **8**(4), 481-487.

